Mode-locking of a terahertz laser by direct phase synchronization

J. Maysonnave,[1] K. Maussang,[1,*] J. R. Freeman,[1] N. Jukam,[1] J. Madéo,[1] P. Cavalié,[1] R. Rungsawang,[1] S.P. Khanna,[2] E.H. Linfield,[2] A.G. Davies,[2] H.E. Beere,[3] D.A. Ritchie,[3] S.S. Dhillon,[1] and J. Tignon[1]

[1]*Laboratoire Pierre Aigrain, Ecole Normale Supérieure, CNRS (UMR 8551), Université P. et M. Curie, Université D. Diderot, 75231 Paris Cedex 05, France*
[2]*School of Electronic and Electrical Engineering, University of Leeds, Leeds LS9 2JT, UK*
[3]*University of Cambridge, Cavendish Laboratory, Cambridge CB3 0HE, UK*
[*]*kenneth.maussang@lpa.ens.fr*

Abstract: A novel scheme to achieve mode-locking of a multimode laser is demonstrated. Traditional methods to produce ultrashort laser pulses are based on modulating the cavity gain or losses at the cavity roundtrip frequency, favoring the pulsed emission. Here, we rather directly act on the phases of the modes, resulting in constructive interference for the appropriated phase relationship. This was performed on a terahertz quantum cascade laser by multimode injection seeding with an external terahertz pulse, resulting in phase mode-locked terahertz laser pulses of 9ps duration, characterized unambiguously in the time domain.

OCIS codes: (140.3520) Lasers, injection-locked; (140.4050) Mode-locked lasers; (140.5965) Semiconductor lasers, quantum cascade; (300.6495) Spectroscopy, terahertz.

References and links

1. L. E. Hargrove, R. L. Fork, and M. A. Pollack, "Locking of He-Ne laser modes induces by synchronous intracavity modulation," Appl. Phys. Lett. **5**(1), 4–5 (1964).
2. E. P. Ippen, C. V. Shank, and A. Dienes, "Passive mode locking of the cw dye laser," Appl. Phys. Lett. **21**(8), 348–350 (1972).
3. A. J. DeMaria, D. A. Stetser, and H. Heynau, "Self mode-locking of lasers with saturable absorbers," Appl. Phys. Lett. **8**(7), 174–176 (1966).
4. U. Keller, "Recent Developments in compact ultrafast lasers," Nature **424**(6950), 831–838 (2003).
5. T. Udem, R. Holzwarth, and T. W. Hänsch, "Optical frequency metrology," Nature **416**(6877), 233–237 (2002).
6. T. Brabec and F. Krausz, "Intense few-cycle laser fields: frontiers of nonlinear optics," Rev. Mod. Phys. **72**(2), 545–591 (2000).
7. D. Mittleman, *Sensing with Terahertz Radiation* (Springer, 2002).
8. M. Tonouchi, "Cutting-edge terahertz technology," Nat. Photonics **1**(2), 97–105 (2007).
9. R. Köhler, A. Tredicucci, F. Beltram, H. E. Beere, E. H. Linfield, A. G. Davies, D. A. Ritchie, R. C. Iotti, and F. Rossi, "Terahertz semiconductor-heterostructure laser," Nature **417**(6885), 156–159 (2002).
10. N. Jukam, S. S. Dhillon, D. Oustinov, J. Madéo, C. Manquest, S. Barbieri, C. Sirtori, S. P. Khanna, E. H. Linfield, A. G. Davies, and J. Tignon, "Terahertz amplifier based on gain switching in a quantum cascade laser," Nat. Photonics **3**(12), 715–719 (2009).
11. D. Oustinov, N. Jukam, R. Rungsawang, J. Madéo, S. Barbieri, P. Filloux, C. Sirtori, X. Marcadet, J. Tignon, and S. S. Dhillon, "Phase seeding of a terahertz quantum cascade laser," Nat. Commun. **1**(6), 69 (2010).
12. S. Barbieri, P. Gellie, G. Santarelli, L. Ding, W. Maineult, C. Sirtori, R. Colombelli, H. Beere, and D. Ritchie, "Phase-locking of a 2.7 THz quantum cascade laser to a mode-locked erbium-doped fibre laser," Nat. Photonics **4**(9), 636–640 (2010).
13. S. Barbieri, M. Ravaro, P. Gellie, G. Santarelli, C. Manquest, C. Sirtori, S. P. Khanna, E. H. Linfield, and A. G. Davies, "Coherent sampling of active mode-locked terahertz quantum cascade lasers and frequency synthesis," Nat. Photonics **5**(5), 306–313 (2011).
14. C. Y. Wang, L. Kuznetsova, V. M. Gkortsas, L. Diehl, F. X. Kärtner, M. A. Belkin, A. Belyanin, X. Li, D. Ham, H. Schneider, P. Grant, C. Y. Song, S. Haffouz, Z. R. Wasilewski, H. C. Liu, and F. Capasso, "Mode-locked pulses from mid-infrared quantum cascade lasers," Opt. Express **17**(15), 12929–12943 (2009).
15. C. A. Schmuttenmaer, "Exploring dynamics in the far-infrared with terahertz spectroscopy," Chem. Rev. **104**(4), 1759–1780 (2004).
16. J. Kröll, J. Darmo, S. S. Dhillon, X. Marcadet, M. Calligaro, C. Sirtori, and K. Unterrainer, "Phase-resolved measurements of stimulated emission in a laser," Nature **449**(7163), 698–701 (2007).

#168168 - $15.00 USD Received 8 May 2012; revised 19 Jul 2012; accepted 20 Jul 2012; published 28 Aug 2012

17. Q. Wu and X.-C. Zhang, "Free-space electro optic sampling of terahertz beams," Appl. Phys. Lett. **67**(24), 3523–3525 (1995).
18. A. Barkan, F. K. Tittel, D. M. Mittleman, R. Dengler, P. H. Siegel, G. Scalari, L. Ajili, J. Faist, H. E. Beere, E. H. Linfield, A. G. Davies, and D. A. Ritchie, "Linewidth and tuning characteristics of terahertz quantum cascade lasers," Opt. Lett. **29**(6), 575–577 (2004).
19. R. P. Green, A. Tredicucci, N. Q. Vinh, B. Murdin, C. Pidgeon, H. E. Beere, and D. A. Ritchie, "Gain recovery dynamics of a terahertz quantum cascade laser," Phys. Rev. B **80**(7), 075303 (2009).
20. J. Madéo, N. Jukam, D. Oustinov, M. Rosticher, R. Rungsawang, J. Tignon, and S. S. Dhillon, "Frequency tunable terahertz interdigitated photoconductive antennas," Electron. Lett. **46**(9), 611–613 (2010).
21. A. Dreyhaupt, S. Winnerl, T. Dekorsy, and M. Helm, "High-intensity terahertz radiation from a microstructured large-area photoconductor," Appl. Phys. Lett. **86**(12), 121114 (2005).
22. D. Turčinková, G. Scalari, F. Castellano, M. I. Amanti, M. Beck, and J. Faist, "Ultra-broadband heterogeneous quantum cascade laser emitting from 2.2 to 3.2 THz," Appl. Phys. Lett. **99**(19), 191104 (2011).
23. H.-T. Chen, W. J. Padilla, M. J. Cich, A. K. Azad, R. D. Averitt, and A. J. Taylor, "A metamaterial solid-state terahertz phase modulator," Nat. Photonics **3**(3), 148–151 (2009).
24. W. S. Warren, H. Rabitz, and M. Dahleh, "Coherent control of quantum dynamics - the dream is alive," Science **259**(5101), 1581–1589 (1993).
25. C. Y. Wang, L. Diehl, A. Gordon, C. Jirauschek, F. X. Kärtner, A. Belyanin, D. Bour, S. Corzine, G. Höfler, M. Troccoli, J. Faist, and F. Capasso, "Coherent instabilities in a semiconductor laser with fast gain recovery," Phys. Rev. A **75**(3), 031802 (2007).
26. A. Gordon, C. Y. Wang, L. Diehl, F. X. Kärtner, A. Belyanin, D. Bour, S. Corzine, G. Höfler, H. C. Liu, H. Schneider, T. Maier, M. Troccoli, J. Faist, and F. Capasso, "Multimode regimes in quantum cascade lasers: From coherent instabilities to spatial hole burning," Phys. Rev. A **77**(5), 053804 (2008).
27. H. Choi, L. Diehl, Z.-K. Wu, M. Giovannini, J. Faist, F. Capasso, and T. B. Norris, "Gain recovery dynamics and photon-driven transport in quantum cascade lasers," Phys. Rev. Lett. **100**(16), 167401 (2008).
28. V. M. Gkortsas, C. Wang, L. Kuznetsova, L. Diehl, A. Gordon, C. Jirauschek, M. A. Belkin, A. Belyanin, F. Capasso, and F. X. Kärtner, "Dynamics of actively mode-locked quantum cascade lasers," Opt. Express **18**(13), 13616–13630 (2010).
29. Y. Silberberg, "Quantum coherent control for nonlinear spectroscopy and microscopy," Annu. Rev. Phys. Chem. **60**(1), 277–292 (2009).

1. Introduction

Ultrashort pulses of light have attracted great interest for decades [1–4], resulting in major fundamental and technological advances, from metrology [5] to industrial applications [4]. They result from the temporal interference between modes that are equally spaced in the frequency domain by the free spectral range (FSR) of a cavity (Fig. 1(a)). For N modes with a random phase relationship, the combined intensity is random as well, with mean amplitude scaling as N (Fig. 1(b), green curve). If, however, the phase difference between consecutive modes is fixed and constant in time, the laser is described as modelocked. The interference is then constructive, leading to the formation of a pulse train with peak intensity scaling as N^2 and period T given by the round trip time (Fig. 1(b), blue curve). The experimental realization of mode-locking is based on two key elements [6]: first, a broadband gain medium that provides a large number of lasing modes leading to shorter pulses (~T/N); second, a mechanism that fixes the phase relationship between lasing modes. This is usually performed through internal modulation of the cavity, either active (e.g. using an acousto-optic modulator) or passive (e.g. the optical Kerr effect). Additionally, the fixed phase relationship may also be disrupted by the group velocity dispersion (GVD) of the medium. This can be compensated to achieve mode-locking by, for example, using an anomalous dispersive element.

Since the original demonstration of mode-locking [1], there has been a constant effort to realize similar schemes in various regions of the electromagnetic spectrum. The terahertz (THz) frequency domain, corresponding to energies in the milli-electronvolt range, has enormous potential for the exploration of intersubband physics in semiconductors, superconductors, imaging, gas analysis or biological applications [7, 8]. In 2002, quantum cascade lasers (QCL) emerge as compact, powerful and efficient sources of THz radiation [9]. Over the past decade, QCL performance has steadily increased to give a far greater range of operating frequencies and higher operating temperatures. More recently, advanced functionalities have been investigated, including pulse amplification [10], phase-control [11, 12], and mode-locking [13, 14] offering the possibility of using QCLs as a powerful and versatile source for time-domain spectroscopy (TDS). Only one realization of mode-locking

#168168 - $15.00 USD Received 8 May 2012; revised 19 Jul 2012; accepted 20 Jul 2012; published 28 Aug 2012

has been reported in the terahertz spectral range, with an active scheme based on frequency feedback [13] but, without direct control over the individual phases.

In the present work, thanks to the unprecedented control over the phase in the THz domain, we demonstrate a novel approach for mode-locking, where the phase of the laser longitudinal modes is directly imprinted using multimode injection seeding [11]. We apply this technique to a 2.75THz quantum cascade laser (QCL), leading to the formation of 9ps THz laser pulses. The unique ability of Time Domain Spectroscopy [15] (TDS) and coherent electro-optic detection [16, 17] to give access to both the amplitude and phase allows to fully characterize the locked phase relationship between the modes, as well as the initial transient laser dynamics.

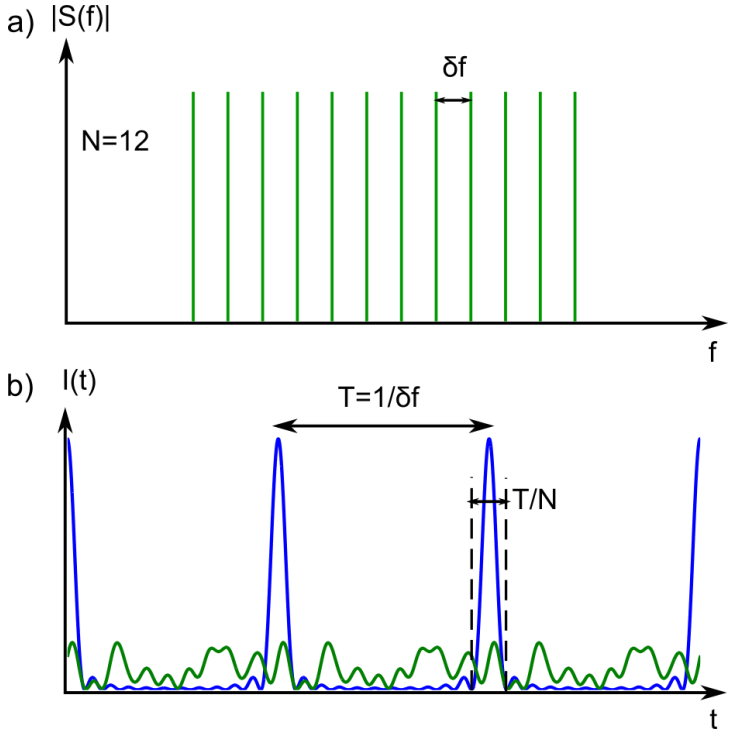

Fig. 1. (a) Frequency domain representation for N = 12 modes with equal amplitude. (b) Corresponding time domain intensity profile. A given amplitude spectrum results in different behaviors in the time domain depending on the phase relationship between modes. The case of mode-locking, where all modes have the same phase, is illustrated in blue, whereas the case of a random phase distribution is shown in green.

2. Phase synchronization by multimode injection seeding

The principle of our experiment is schematically depicted in Fig. 2 and satisfies the two key requirements cited above. Firstly, we use a QCL with a 150GHz gain bandwidth, able to sustain about 11 lasing modes. Secondly, the phase of the QCL lasing modes is initially fixed by an external seed with a known phase rather than set randomly by the inherent spontaneous emission [11]. For this, the QCL is switched-on periodically and synchronously injected with broadband phase-locked THz seed pulses that have a constant phase over the QCL gain bandwidth [15]. This multimode injection seeding induces the formation of multiple longitudinal modes lasing with the fixed phase relationship of the seed. As a result, after a brief linear amplification regime, the gain is clamped to the losses, leading to the formation of a train of THz laser pulses with constant amplitude (Fig. 2(a)). Moreover, the QCL is periodically switched on and off, on a nanosecond timescale so that, as it will be demonstrated below, the dispersion remains negligible. This periodic switching is performed

#168168 - $15.00 USD Received 8 May 2012; revised 19 Jul 2012; accepted 20 Jul 2012; published 28 Aug 2012

synchronously with the seeding, leading to a series of pulse trains, synchronized and phase-locked to each other.

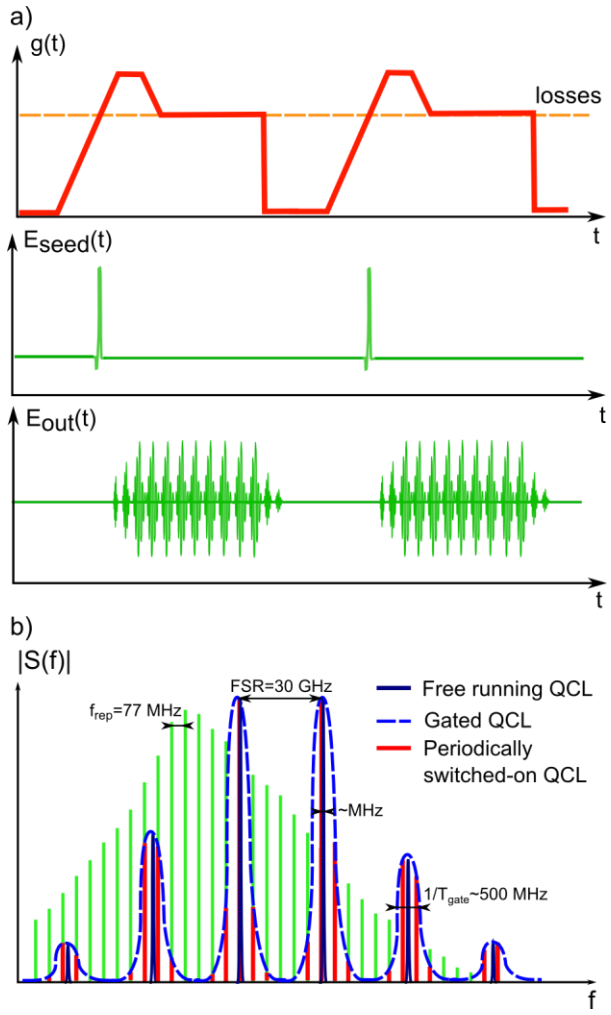

Fig. 2. (a) Time domain: the QCL is gated at low frequency compared to the roundtrip time. When the laser is switched on, a seeding pulse is injected in the cavity with a field $E_{seed}(t)$. After a brief transient regime, the laser gain g(t) is saturated and matches the losses, leading to an output field $E_{out}(t)$ consisting in a constant amplitude laser pulse train. (b) Frequency domain: the terahertz seed pulses consist in a frequency comb with spacing f_{rep} and no frequency offset (green full lines). The free running QCL modes have linewidths smaller than f_{rep} (blue full lines) and a priori do not match the excitation comb frequencies. When the laser is gated for $T_{gate} < 1/f_{rep}$, lines are broadened up to $1/T_{gate}$ with overlap over several frequencies of the excitation comb (blue dashed lines). If the laser is gated periodically at f_{rep} frequency, an inner comb structure appears, with f_{rep} spacing and no frequency offset (red full lines). Each component of the periodically gated QCL spectrum is then excited by a component of the excitation terahertz frequency comb, imprinting its phase.

The periodic switching also plays an important role for the resonant injection of the QCL laser modes, as can be understood in the frequency domain (Fig. 2(b)). The seed field consists in a series of identical THz pulses with a repetition rate f_{rep} (76MHz). As a result, the seed spectrum is a frequency comb, with spacing f_{rep} (Fig. 2(c), green lines) and no frequency offset since the carrier phase shift is null [5]. The free-running QCL spectrum displays several modes, spaced by the FSR, with a linewidth in the MHz range [18] (blue solid lines). Consequently, the seed pulse frequency components are a priori not resonant with the free-

#168168 - $15.00 USD Received 8 May 2012; revised 19 Jul 2012; accepted 20 Jul 2012; published 28 Aug 2012

running QCL modes. However, when the QCL is turned-on for a time $T_{gate}<1/f_{rep}$, each QCL mode broadens to a linewidth T_{gate} (blue dashed lines), larger than the excitation comb frequency spacing. Last, since the QCL is periodically turned-on with a gate synchronized to seeding pulses, the spectrum of the broadened QCL is structured into a comb with spacing f_{rep} and no frequency offset (red lines). Therefore each component of the periodically gated QCL spectrum is resonantly excited by a component of the seeding terahertz frequency comb, imprinting its own phase and permitting multi-mode injection seeding.

3. Experimental setup

A schematic diagram of the experiment is shown in Fig. 3. To produce stable pulse in time by mode-locking, the gain recovery time (typically 50ps in THz QCLs) has to be longer than the cavity round trip time [19]. Thus, the laser cavity has to be short enough to ensure this condition is satisfied, but also long enough to obtain several lasing modes. As a compromise, the QCL is cleaved to a length of 1.5mm which provides a round trip time of 35ps and a mode spacing of 29GHz. The QCL is an AlGaAs/GaAs bound-to-continuum design with a plasmon waveguide that lases at 2.75THz with a 150GHz bandwidth, and typically ~20mW output power in free running operation. It is soldered with indium onto a copper heat sink which is maintained at a temperature of 10K. An upper limit of the GVD was estimated to be $4\cdot10^{-2}$ ps^2/mm at 3THz. Thus, a gaussian pulse of 10ps FWHM broadens by one cycle (333fs) only after 3ns of propagation. Consequently, the QCL is switched-on for less than 1ns to avoid any dispersion effects.

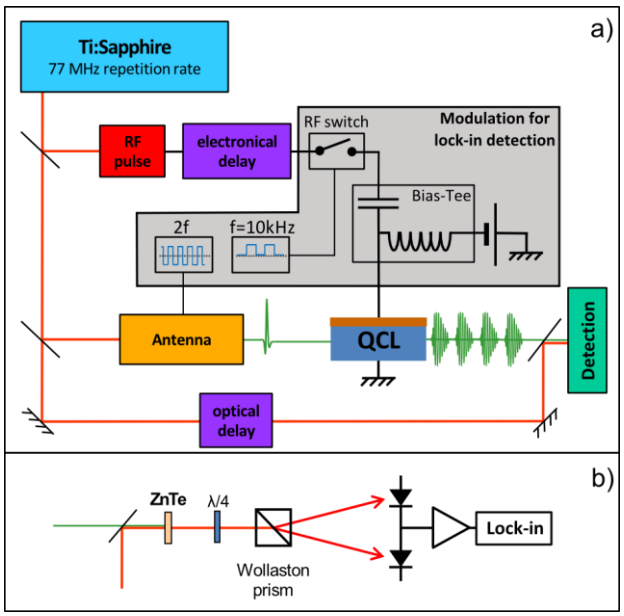

Fig. 3. (a) The seed THz pulses are produced by illuminating an interdigited photo-conductive antenna with near infrared femtosecond laser pulses. After a THz seed pulse enters the QCL, a square RF pulse synchronized to the femtosecond laser pulse biases the QCL above lasing threshold. The THz beam emitted and a split-off beam from the femtosecond beam are then focused onto a ZnTe crystal for the electro-optic sampling detection. (b) Detection of the emitted field, with a quarter wave electro-optic sampling geometry. The signal is proportional to the amplitude of THz field emitted by the QCL.

A RF signal consisting of 1ns long square pulses with a period of 13ns is generated by illuminating a photodiode with a Ti:Sapphire femtosecond laser, with pulse duration of typically 100fs and a repetition rate of 76MHz. This periodically biases the QCL above lasing threshold [11], when added to a quasi-DC bias (25% duty cycle at kHz frequencies) with a bias tee. The RF pulse rise time is typically 400ps with duration of 600ps; the laser turn-on is

#168168 - $15.00 USD Received 8 May 2012; revised 19 Jul 2012; accepted 20 Jul 2012; published 28 Aug 2012

determined by the rise time of the RF pulse. A 50Ω RF switch modulates this bias for lock-in detection.

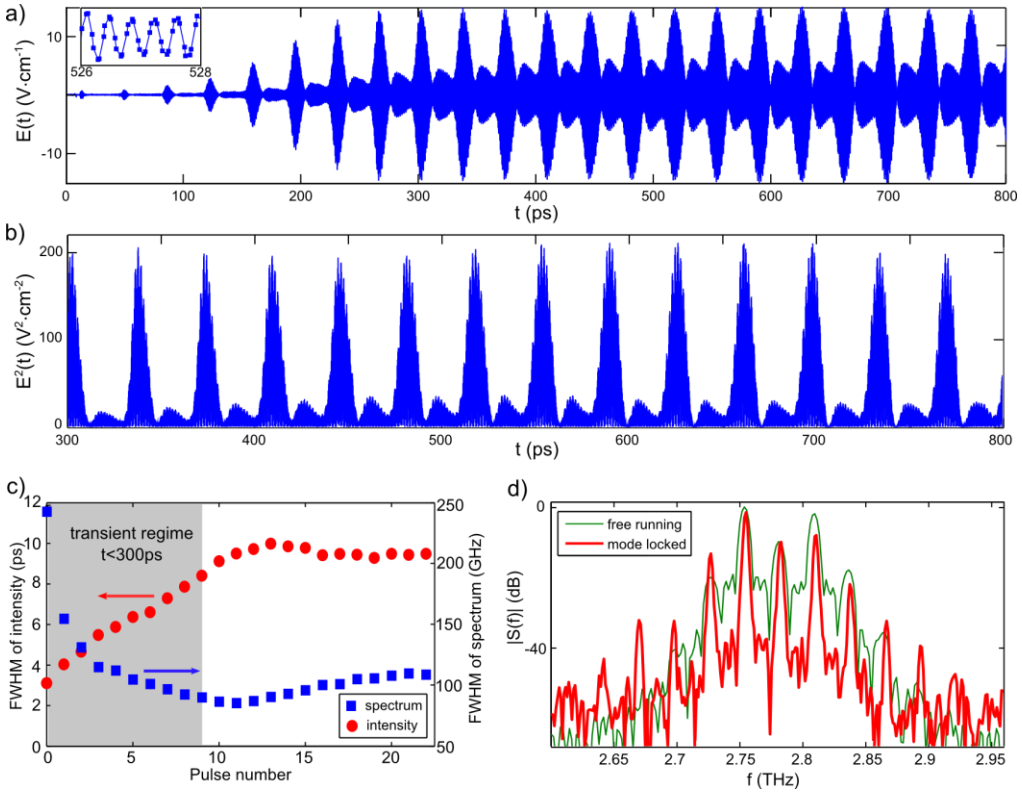

Fig. 4. (a) Amplitude and phase resolved measurements of the emitted electric field, for a THz seed pulse generated with 4V applied to the photo-conductive antenna. A DC bias of 120A/cm^2 and 7.5W RF pulse is applied to the QCL, equivalent to adding around 129A/cm^2. The laser threshold is 167A/cm^2. The seeding pulse is injected in the QCL at t = –24ps. Inset: expanded view of the TDS measurement between t = 526ps and t = 528ps. (b) Instantaneous emitted intensity, calculated from the TDS field measurement. A train of pulses, separated by the cavity round trip (35ps), is clearly visible, with a FWHM of 9ps in intensity. (c) Pulse width (blue square, right axis) and spectrum width (red circle, left axis) as a function of the number of round trips in the QCL. (d) Fourier transform of the measured electrical field in the steady state regime. Several modes are visible, separated by the cavity free spectral range (29GHz). A spectrum of the free running QCL, obtained by Fourier transform infrared spectroscopy (FTIR), has been superimposed. Both are renormalized to their maximum value and are resolution limited.

The THz seed pulses are generated with a photo-conductive antenna [20, 21], excited by the same laser, and are coupled into the facet of the QCL with parabolic mirrors (not shown). An electronic delay on the RF pulse permits synchronization with the seeding pulse. The value of the quasi-DC bias applied on the laser is not critical to achieve the injection seeding. The antenna is biased periodically at frequency 2f with a constant polarity. The QCL is modulated at frequency f = 10kHz, while the lock-in reference is f, so that in this configuration only the field emitted by the QCL is detected. The THz beam emitted and a split-off beam from the femtosecond beam are then focused onto a 200µm ZnTe crystal for the electro-optic sampling detection [17] (Fig. 3(b)): the THz electric field induces a small birefringence and a polarization rotation of the femtosecond beam, measured in a balanced photodiode scheme. It results in a direct measurement of the field amplitude and phase, including any transient dynamics.

#168168 - $15.00 USD Received 8 May 2012; revised 19 Jul 2012; accepted 20 Jul 2012; published 28 Aug 2012

4. Results

Figure 4(a) shows the amplitude of electrical field E(t) emitted by the QCL, and demonstrates unambiguously the formation of ultrashort THz laser pulses. At early times (t<300ps), the frequency components of the seed pulse corresponding to the QCL gain bandwidth are amplified, while the rest undergo losses and rapidly vanish, resulting in a spectral narrowing (blue squares in Fig. 4(c)). In the time domain, this results in pulse width broadening (red circles in Fig. 4(c)). After this transient regime of about 300ps, a quasi-constant amplitude train of pulses is clearly visible, with a FWHM of about 9ps in intensity, as illustrated more clearly by Fig. 4(b) which shows the square of the electric field $E^2(t)$. Figure 4(d) shows the spectrum obtained by Fourier transform of the signal measured in the steady state region (red curve). It is obtained by weighting the signal with a hamming window of 500ps centered at t_0 = 550ps, and the FFT routine of MATLAB is used to compute the spectrum. It consists of an ensemble of discrete modes, equally spaced by the QCL FSR (29GHz). The resolution of the measurement is limited by the length of the mechanical delay line (800ps) that does not allow the resolution of the underlying QCL frequency comb discussed above. The spectrum of the free-running QCL (i.e. without seeding and RF modulation), which cannot be determined using electro-optic sampling, was measured with a commercial FTIR and is also shown in Fig. 4(d) (resolution limited). While the center frequencies have similar relative amplitudes, the spectrum of the injected QCL presents additional lasing side-modes, interpreted as a signature of mode-locking [14].

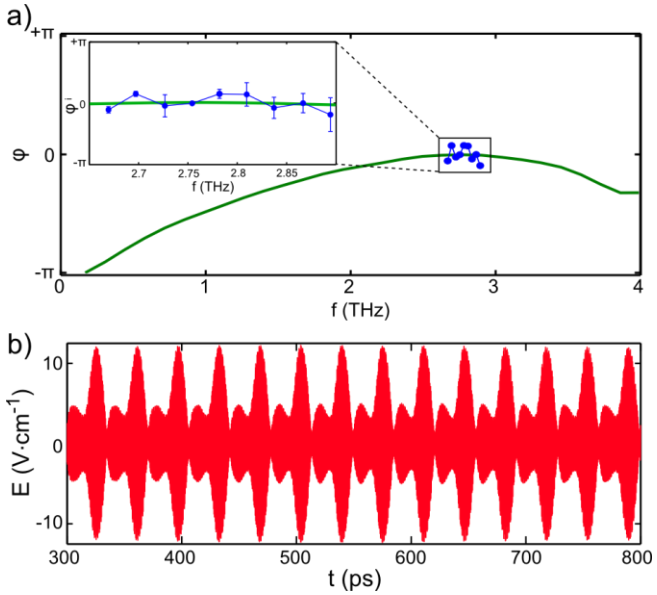

Fig. 5. (a) The phase of each laser mode (in blue) is obtained from the argument of the complex FFT of the field measured in the steady state region (t>300ps). Similarly, a measurement of the seeding pulse field provide after FFT the spectral phase of the seeding pulse (green line). In the inset, an expanded view for clarity, around the laser modes' frequencies, showing unambiguously that the phases are identical. The spectral phase of the seeding pulse has negligible variation over the frequency bandwidth of the laser ($2\pi \times 6 \cdot 10^{-3}$ rad standard deviation). (b) Reconstructed field from the measured amplitudes and phases.

The spectral phase of the field can be obtained from the argument of the complex spectrum at the corresponding frequency, but for a window of 400ps only, centered at t_0 = 550ps. Error bars are estimated by measuring the phase with the same procedure but for different values of t_0 from 500ps to 600ps. Then, the phase of each mode can be extracted (Fig. 5(a), blue dots) and compared to the spectral phase of the seeding pulse (Fig. 5(a), green line). They are measured to be almost identical within the error bars. This clearly

#168168 - $15.00 USD Received 8 May 2012; revised 19 Jul 2012; accepted 20 Jul 2012; published 28 Aug 2012

demonstrates that (i) there is a fixed phase relationship between all the modes, imprinted by the seeding, and (ii) the phase difference between the modes is constant, providing optimal contrast for the interference and hence Fourier-transform limited pulses [6]. As a last demonstration of the completeness of the measurement, we show in Fig. 5(b) the field calculated from the measured amplitudes and phases (t>300ps), showing excellent agreement with the measured field (Fig. 4(a)). The dependence of mode-locking on quasi-DC point of the laser has been investigated, but no clear behavior has been observed.

5. Conclusion and outlook

In this current work, 9ps THz pulses are generated, limited by the number of modes i.e. the spectral gain of the laser. A longer cavity would increase the number of modes leading to shorter pulses, but it would also increase the cavity round trip time, so that the mode-locked solution might not be stable. However, in order to obtain shorter pulses, it would be very interesting to use broadband QCLs that have shown bandwidths greater than 1THz [22]. Further, new THz phase-modulation techniques [23] could be used to finely adjust the individual phases of the mode phases with on-demand values. This would provide an integrated pulse shaper, whereas in optics, pulse shaping is a subsequent [24]. In conclusion, we have shown that mode-locking can be achieved by directly imprinting the desired phase relationship onto the laser modes of a THz QCL by multimode phase-locked injection seeding, directly characterized with phase resolved electro-optic detection. By increasing the pulse duration of the RF signal used to switch on the QCL, one could perform experimental investigations of pulse formation dynamics and stability in QCLs [25–28], and ultimately the generation of ultrashort and intense THz pulses. Such devices would also be powerful tools for use in THz-TDS, molecular spectroscopy or coherent control with phase-shaped pulses [24, 29].

Acknowledgments

We thank Louis-Anne de Vaulchier and François-Régis Jasnot, who performed the FTIR measurement. We acknowledge funding from ANR (FR), EPSRC (UK), and European Research Council grants “TOSCA” and “NOTES”.